mathematics

MDPI

Article

Variable Gap MAG Welding Penetration Control Using Rough Set Knowledge Acquisition

Zhiqiang Feng [1,*], Hao Yuan [1], Junfeng Han [1], Na Lv [2], Xin Li [1] and Quan Li [1]

[1] School of Mechanical and Marine Engineering, Beibu Gulf University, Qinzhou 535011, China; 2002011131@stu.bbgu.edu.cn (H.Y.); hanjf@bbgu.edu.cn (J.H.); lxin@bbgu.edu.cn (X.L.); liquan@bbgu.edu.cn (Q.L.)

[2] School of Materials Science and Engineering, Shanghai Jiao Tong University, Shanghai 200240, China; nana414526@sjtu.edu.cn

* Correspondence: fzqsjtu@163.com

Abstract: The establishment of the correspondence between the important features of the topside weld pool and the penetration state is a key link in penetration control. This article presents a scheme of variable gap welding penetration control based on rough-fuzzy modeling. By utilizing the basic concepts of variable precision rough sets and conditional information entropy, relevant algorithms for attribute reduction and rule extraction in decision information systems are addressed. Raw data for modeling are obtained through current–gap combination experiments, and then rough-set-based knowledge acquisition algorithms are used to generate classification rules for the penetration state. Based on the correspondence between the important features of the topside pool and the penetration state, a fuzzy control model is established. Welding experiments under variable gaps are conducted to examine the proposed control scheme, and the results indicate that the weld has good penetration and meets the requirements of welding specifications.

Keywords: rough set; knowledge acquisition; penetration control; fuzzy modeling; weld gap

MSC: 68T35

check for updates

Citation: Feng, Z.; Yuan, H.; Han, J.; Lv, N.; Li, X.; Li, Q. Variable Gap MAG Welding Penetration Control Using Rough Set Knowledge Acquisition. *Mathematics* **2023**, *11*, 4504. https://doi.org/10.3390/math11214504

Academic Editor: Óscar Valero Sierra

Received: 24 September 2023
Revised: 24 October 2023
Accepted: 30 October 2023
Published: 31 October 2023

Copyright: © 2023 by the authors. Licensee MDPI, Basel, Switzerland. This article is an open access article distributed under the terms and conditions of the Creative Commons Attribution (CC BY) license (https://creativecommons.org/licenses/by/4.0/).

1. Introduction

Metal active gas (MAG) welding is widely used in industries such as aviation, shipbuilding, chemical, construction, and mechanical manufacturing [1]. Penetration control is a key technology in MAG one-side welding with back formation. The weld gap is one of the important process parameters that affect the penetration state of the weld seam. The main function of a welding fit-up gap is to ensure root penetration, so its size should comply with the welding specifications and maintain uniformity and consistency. If the gap is too small, the weldment cannot be fully welded through; if it is too large, it leads to over-penetration, collapse, and even burning through. In practical applications, due to the influence of weldment processing and assembly, it is often difficult to ensure the uniform and consistent size of weld gaps. Therefore, using constant-specification welding will lead to poor penetration of the weld seam. With the development of machine vision, image processing, and artificial intelligence technologies, using intelligent means to control the shape and size of the welding pool has become one of the main ways to achieve welding penetration control [2,3].

The back width of the weld seam can directly characterize the penetration state. However, due to various limitations, it is impossible to directly observe the backside of the weld in most cases, such as the welding of closed or semi-closed structures. A large amount of engineering practice and welders' experience has shown that there is a certain relationship between the topside shape of the molten pool and the penetration state. Therefore, the current main approach for welding penetration control is to establish a

welding process model that reflects the relationship between the topside characteristics of the weld pool and the penetration state. During the welding process, the penetration state is predicted by detecting the topside shape of the weld pool, and then real-time control for the back width of the weld is achieved by adjusting welding specification parameters.

The development of welding process modeling has gone through a process from simple to complex. The experimental results indicate that the more abundant the obtained topside shape information of the molten pool, the more accurate the prediction results of the penetration state. As a result, some researchers propose to establish a multi-input welding process model by integrating more feature information (such as weld pool width, length, area, tail width, trailing angle, etc.), and further developing a model that combines weld pool feature information, welding specifications, and welding process conditions (such as the fit-up gap) to predict the back width of the weld seam [4].

With the increase in the input feature information, the prediction accuracy of the welding process model has improved to a certain extent. However, high-dimensional inputs inevitably generate redundant features and a large amount of redundant information, which makes the model more complex and makes it difficult to obtain the regularity of penetration status changing with the topside features of the molten pool through data analysis and processing. It is worth noting that during the welding process, experienced welders often determine the penetration state by observing the important features of the topside molten pool, and then adjust parameters such as welding current and welding speed to ensure weld penetration. Therefore, in the automated welding process, finding important features that can characterize the penetration state from the frontal image of the molten pool is of great significance for achieving intelligent control of penetration.

Rough set (RS) theory is a mathematical tool for data representation, learning, and induction, which has been widely applied in fields such as knowledge discovery, machine learning, pattern recognition, and decision support [5–8]. The core idea of rough sets is to acquire decision or classification rules through knowledge reduction under the condition that maintains the system's classification ability unchanged. Therefore, if the rough set method is used to establish the correspondence between the important features of the topside melt pool and the penetration state, then the penetration prediction process can be avoided in closed-loop control, and penetration control is achieved by adjusting the topside shape of the melt pool.

The organizational structure of the rest of this article is as follows. Section 2 briefly reviews the relevant work of fuzzy logic control in welding and other engineering fields. Section 3 describes the relevant algorithms based on variable precision rough set (VPRS) knowledge acquisition and then proposes a rough-fuzzy control scheme for the variable gap welding penetration process. Section 4 presents and discusses the relevant results of using the proposed penetration control scheme through variable gap mild steel MAG welding experiments. Section 5 describes the conclusion of this article.

2. Literature Review

Welding penetration is one of the most important technical requirements for load-bearing welds, and the control of the penetration process has always been a concern in the welding industry [9,10]. In terms of control strategies for the penetration status, the main algorithms include fuzzy logic control, fuzzy neural network control, adaptive control, etc.

As a powerful tool for describing human thinking in dealing with imprecise and uncertain problems, fuzzy theory has been widely applied in the fields of decision-making and control [11–14]. Fuzzy logic control has the advantages of flexibility, simplicity, and strong robustness, with strong adaptability to complex nonlinear systems. Ref. [15] selected a fuzzy control strategy for the design of a permanent magnet synchronous motor controller and used a heuristic global optimization algorithm to optimize the weights of the fuzzy controller rules. The experimental results showed that the controller had good control performance under load disturbances. Ref. [16] used fuzzy logic to design an automatic transmission control system to meet the requirements of lower jerk response, smoother

driving comfort, and lower fuel consumption during vehicle driving. Ref. [17] proposed a novel fuzzy logic control scheme for tracking the joint trajectory of robot manipulators, which took acceleration as one of its language variables. The results of the system simulation experiments indicated that the addition of fuzzy variable acceleration significantly improved the system's response.

In the field of welding, fuzzy logic technology has been applied to weld seam tracking and welding forming control. Refs. [18–20] presented a fuzzy-logic-based adaptive control scheme, where the membership functions of input and output variables could be adaptively adjusted according to the tracking state. The experimental results showed that the proposed scheme had high seam-tracking accuracy and better performance than traditional seam-tracking controllers. To eliminate errors and suppress overshoot, [21,22] designed a hybrid controller that combined fuzzy logic control with proportional integral or proportional control. Simulation results showed that the scheme could achieve fast and accurate tracking of welds. Ref. [23] adopted a fuzzy control model to simulate external disturbance signals and dynamic uncertainty signals, which enabled the controller to effectively suppress chattering caused by sliding mode control algorithms. The experiments indicated that this model effectively achieved the tracking of welding robots.

Regarding the control of weld formation, [24] introduced the application of fuzzy logic in welding process control. A fuzzy control model for weld pool width was established based on the proportional relationship between the topside width of the weld pool and the depth of the weld pool. During the welding process, fuzzy inference was used to adjust the welding parameters according to the detected width of the molten pool, thereby achieving online control of the penetration depth. Ref. [25] focused on the problem of online control of fusion penetration. Based on experimental data, a fuzzy identification method was used to extract fuzzy control rules for the welding process, and a fuzzy controller with self-learning adaptability was designed. The experimental results indicated that the controller had an intelligent control effect. Ref. [26] established a fuzzy control system with wire feeding speed as the control variable and surface melt hole size as the controlled variable. The experimental results showed that the welding seam formed well under variable gap conditions. Ref. [27] used a fuzzy control algorithm to automatically adjust the downward pressure of the welding device. Through MATLAB simulation experiments, it was verified that the fuzzy control algorithm could effectively control the welding pressure of the welding device, which helped to improve the quality of weld forming.

In addition to fuzzy-logic-based control methods, some researchers have investigated adaptive control methods for welding penetration. Ref. [28] used the Hammerstein model to describe nonlinear systems and identified model parameters online through the recursive least-squares method to achieve adaptive control of the welding process. Ref. [29] established a penetration state prediction model based on the characteristics of molten pool images and designed a penetration model-free adaptive controller. The controller was validated through variable heat dissipation and variable plate thickness welding experiments.

3. Methods

3.1. VPRS-Based Knowledge Acquisition

3.1.1. Preliminaries

The classification of classical rough set processing is a precise classification based on the "completely belonging" or "not belonging" relationship. However, in practical applications, interference such as noise is often unavoidable, which makes it difficult for the classification performance of classical rough sets to achieve the expected results. To enhance the anti-interference ability of the classical model, Ziarko et al. proposed an extended rough set model called the variable precision rough set (VPRS) [30].

Let U be a nonempty finite universe. Given a binary function $\kappa : U \times U \to [0,1]$ such that

$$\kappa(X,Y) = \begin{cases} \frac{\text{card}(X \cap Y)}{\text{card}(X)}, X \neq \varnothing \\ 1, X = \varnothing \end{cases} \quad (1)$$

holds for any $X, Y \subseteq U$, where $\mathrm{card}(\cdot)$ is the cardinal number of a set, then $\kappa(X, Y)$ is called the relative correct classification rate of X with respect to Y.

Suppose $(U, C \cup \{d\})$ is a decision information system, where C is the conditional attribute set and d is the decision attribute. $X_i (i = 1, 2, \cdots, m)$ is the conditional class derived from partition U/C, and $Y_j (j = 1, 2, \cdots, n)$ is the decision class derived from partition U/d. Given $\beta \in (0.5, 1]$, the β-lower approximation of Y_j with respect to C is

$$\underline{C}^{\beta}(Y_j) = \{X_i \in U/C : \kappa(X_i, Y_j) \geq \beta\}. \tag{2}$$

The β-positive region of d with respect to C is

$$POS_C^{\beta}(d) = \bigcup_{Y_j \in \mathbb{U}/d} \underline{C}^{\beta}(Y_j) \tag{3}$$

and the β-approximate classification quality of d with respect to C is

$$\gamma_C^{\beta}(d) = \mathrm{card}(POS_C^{\beta}(d))/\mathrm{card}(U). \tag{4}$$

From Formula (4), it can be seen that the approximate classification quality reflects the proportion of objects assigned from conditional class U/C to decision class U/d in the universe U for a given threshold value β.

Definition 1 ([30]). *Let $(U, C \cup \{d\})$ be a decision information system and $\beta \in (0.5, 1]$. For any $B \subseteq C$, if:*

$$\begin{cases} 1)\gamma_B^{\beta}(d) = \gamma_C^{\beta}(d) \\ 2)\forall a \in B,\ \gamma_{B-\{a\}}^{\beta}(d) \neq \gamma_C^{\beta}(d) \end{cases} \tag{5}$$

holds, then B is called a β-approximate reduction of C with respect to d, denoted as $RED_d^{\beta}(C)$.

The above definition indicates that the approximate classification quality of a minimal attribute subset B in a conditional attribute set C for decision attribute d is equal to that of C for d.

Attribute significance is a key concept in rough set knowledge reduction. In the algebraic view of rough set theory, whether a conditional attribute is reducible depends on whether the lower approximation set of the decision set is changed after deleting the conditional attribute, that is, whether it has an impact on the deterministic (compatible) part of the decision information. Thus, a definition of attribute significance based on approximate classification quality is as follows.

Definition 2 ([31]). *Let $(U, C \cup \{d\})$ be a decision information system and $\beta \in (0.5, 1]$. For any $a \in C$, the significance of a relative to d in C is expressed as*

$$SIG(a, C, d) = \gamma_C^{\beta}(d) - \gamma_{C-\{a\}}^{\beta}(d). \tag{6}$$

Formula (6) reflects the changes in the approximate classification quality caused by removing a from the conditional attribute set C. If $SIG(a, C, d)$ is equal to 0, then a is unimportant(redundant) in C with respect to d; otherwise, a is irreducible.

3.1.2. Attribute Reduction and Rules Extraction

Rough set has the ability to automatically acquire knowledge from an original data set. It does not require any prior knowledge and generates a set of production rules in the form of "if ... then ..." from a decision information system through attribute reduction and rule extraction.

Attribute reduction is a core part of rough set theory, which requires retaining necessary and important conditional attributes or eliminating redundant and unimportant

conditional attributes while maintaining unchanged the ability of the conditional attributes to classify the decision attributes.

Rough-set-based attribute reduction can be divided into theoretical algorithms and heuristic algorithms according to whether heuristic information is utilized or not. For theoretical reduction algorithms, it is difficult to seek a minimal or optimal reduction of an information system due to the combinatorial explosion problem of attributes. Therefore, heuristic algorithms are generally used to obtain approximate optimal or suboptimal solutions.

The reduction strategy of heuristic algorithms is how to select conditional attributes, while the selection order is determined using the importance of attributes in the decision information system. The description of attribute significance mainly includes the algebraic-view-based definition (see Definition 2) and the information-view-based definition [31]. In the information view of rough set theory, whether a conditional attribute is reducible depends on whether the conditional information entropy of the decision information system is changed after deleting the conditional attribute. The information entropy of the system is generated by the uncertain (incompatible) part, and the information entropy of the deterministic (compatible) part is 0. That is to say, if deleting an attribute neither affects the probability distribution of the uncertain part nor changes the classification of the deterministic part, then the attribute is unimportant (redundant). Thus, it can be seen that the information definition of attribute importance includes its algebraic definition. The significance of attributes based on conditional information entropy is defined as follows.

Definition 3. Let $(U, C \cup \{d\})$ *be a decision information system and* $\beta \in (0.5, 1]$. *For any* $a \in C$, *the significance of* a *relative to* d *in* C *is expressed as*

$$SIG(a, C, d) = H(d|C - \{a\}) - H(d|C) \tag{7}$$

where $H(d|C - \{a\})$ *and* $H(d|C)$ *are the conditional entropy of* d *with respect to* $C - \{a\}$ *and* C, *respectively.*

Based on Definitions 1 and 3, a rapid reduction of conditional attributes in decision information systems can be achieved. The basic idea of this algorithm is to sort all conditional attributes in the decision information system in descending order of significance and then sequentially add them to the reduction set RED until the termination conditions of the algorithm are met. The algorithm uses the importance of attributes based on conditional entropy as heuristic information and believes that the greater the importance of the attributes, the greater their classification ability. Thus, a rapid increase in classification quality can be achieved by adding those important attributes one by one.

Algorithm 1: Attribute significance-based approximate reduction (ASBAR).

Input: $(U, C \cup \{d\}), \beta$
Output: Reduction set RED
Step 1. Calculate the classification quality γ_C^β of C according to Formula (4).
Step 2. Calculate the attribute significance $SIG(a, C, d)$ for every $a \in C$ according to Formula (7).
Step 3. $RED \leftarrow \varnothing$, repeat the following operations for every $a \in C$ in descending order of $SIG(a, C, d)$.
Step 3.1. $RED \leftarrow RED \cup \{a\}$, calculate the classification quality γ_{RED}^β of RED according to Formula (4).
Step 3.2. If $\gamma_{RED}^\beta = \gamma_C^\beta$, output RED; otherwise, proceed to Step 3.1.

In addition to providing methods for attribute (knowledge) reduction in decision information systems, rough set theory also has the ability to extract decision or classification rules in the form of "if ... then ..." from decision information systems.

Let $(U, RED \cup \{d\})$ be a reduced decision information system and $X_i (i = 1, 2, \cdots, l)$ and $Y_j (j = 1, 2, \cdots, s)$ be the conditional class and decision class derived from the partitions

U/RED and $U/\{d\}$, respectively. For any $x \in X_i$ and $x \in Y_j$, the descriptions of X_i and Y_j in $(U, RED \cup \{d\})$ are

$$\begin{cases} \mathrm{Des}(X_i) = \underset{a \in RED}{\wedge}(a = a(x)) \\ \mathrm{Des}(Y_j) = (d = d(x)) \end{cases} \tag{8}$$

where $a(x)$ and $d(x)$ are the attribute values of a and d with regard to x, respectively. The decision or classification rule R_x generated by $(U, RED \cup \{d\})$ with regard to x can be expressed as

$$R_x : \ \mathrm{Des}(X_i) \rightarrow \mathrm{Des}(Y_j)(\mathrm{conf}_{ij}) \tag{9}$$

where $\mathrm{Des}(X_i)$ and $\mathrm{Des}(Y_j)$ are the antecedent part and the consequent part of the rule, respectively. The confidence degree conf_{ij} of the rule is obtained by

$$\mathrm{conf}_{ij} = \frac{\mathrm{card}(X_i \cap Y_j)}{\mathrm{card}(X_i)}. \tag{10}$$

Algorithm 2: Confidence-based rule extraction (CBRE).

Input: $(U, RED \cup \{d\})$, threshold λ
Output: Rule set R_S
Step 1. Initialize $R_S \leftarrow \varnothing$, $U/RED = \{X_1, X_2, \cdots, X_l\}$, $U/\{d\} = \{Y_1, Y_2, \cdots, Y_s\}$.
Step 2. For $i = 1$ to l
  Step 2.1. For $j = 1$ to s
    Step 2.1.1. Calculate conf_{ij} according to Formula (10).
    Step 2.1.2. If $\mathrm{conf}_{ij} \geq \lambda$, then $R_S \leftarrow R_S \cup \left\{\mathrm{Des}(X_i) \rightarrow \mathrm{Des}(Y_j)(\mathrm{conf}_{ij})\right\}$.
  Step 3. Output R_S.

3.2. Proposed Control Scheme

An effective way to achieve welding penetration control is to simulate the observation, judgment, and operation behavior of welders on the welding pool through intelligent means. In this subsection, a rough-fuzzy control scheme for variable gap welding penetration is proposed by combining rough set knowledge acquisition with fuzzy logic modeling. First, the original data are obtained by using visual sensing and image processing through the $I \times G$ combination welding experiment. Then, the VPRS-based knowledge acquisition algorithm is used to obtain the corresponding relationship between the topside features of the molten pool and the penetration state, thereby establishing a fuzzy control model for the topside parameters of the weld pool. Finally, welding penetration control under variable gap conditions is achieved through the inference and judgment of the model. The basic flow of the proposed control scheme is shown in Figure 1, where D, $y(t)$, $e(t)$, and $u(t)$ represent expected values, measured values, errors, and control quantities, respectively.

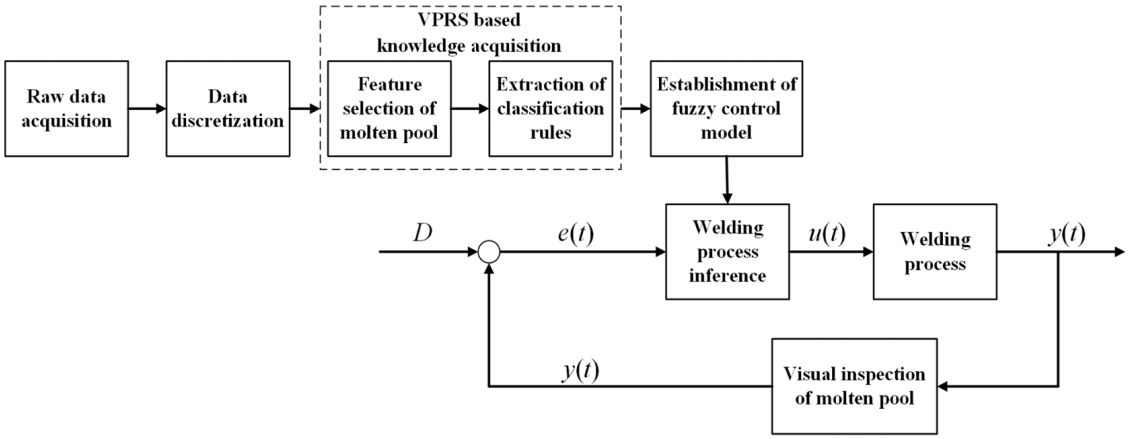


Figure 1. Basic flow of rough-fuzzy control scheme for variable gap welding penetration.

4. Results and Discussion

4.1. Establishment of Dataset

The welding current is one of the main specification parameters that affect the topside shape and penetration state of the weld pool. To establish a decision information system that describes the relationships between the topside features of the molten pool and the penetration state under different current and gap conditions, the $I \times G$ combination welding experiments are conducted using the MAG welding experimental platform. A mild steel test piece is used with a specification of 300 × 150 × 6 mm^3. The joint type is butt with a 60° Y-shaped groove and a root face of 1.5 mm. Mild steel wire (1.2 mm diameter) is used, with an 80% Ar–20% CO_2 shielding gas and a gas flow rate of 15 L/min. The welding speed is approximately 47 cm/min; the arc voltage is set at approximately 21 V; the welding current I = {155, 165, 185, 205, 215} A; and the root gap G = {0.4, 0.7, 1.2, 1.7, 2.0} mm. After welding is completed, we measure the back width W_B of each weld seam (excluding the burn-through state).

The weld pool images in various penetration states are processed through processing steps such as filtering denoising, threshold segmentation, and edge detection to obtain their corresponding molten pool contours. Figure 2 shows the topside images and contours of the pool under three different penetration states: incomplete penetration, full penetration, and over-penetration, where $I \times G$ is taken as (165, 0.4), (185, 1.2), and (205, 1.7), respectively.

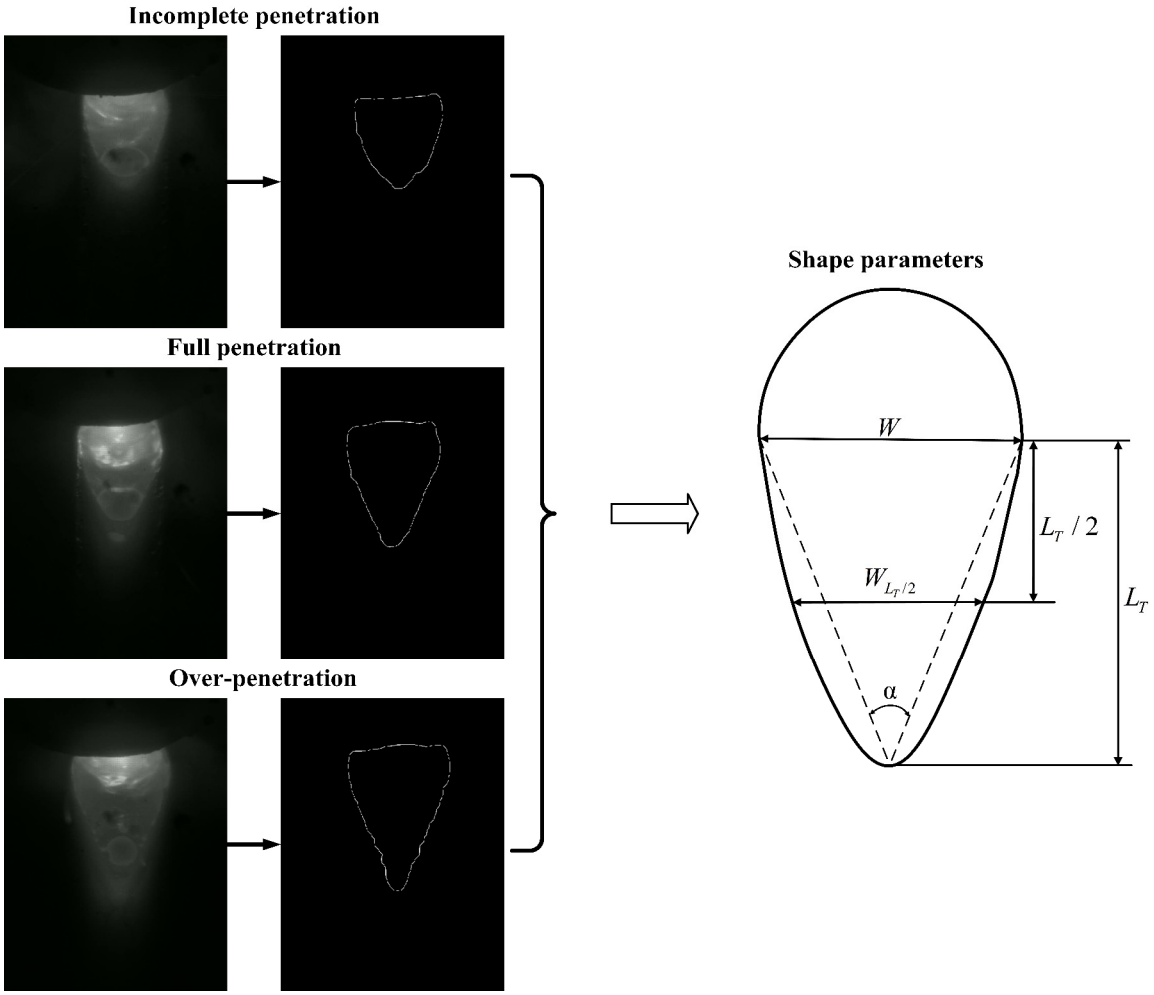


Figure 2. Topside contour of welding pool and its shape parameters.

From Figure 2, it can be seen that compared with the incomplete penetration status, the tail of the molten pool in the fully penetrated state becomes larger, with longer and sharper shapes. This is because, as the welding current increases, the geometric parameters

such as the half-length, width, and tail area of the weld pool tend to increase. Additionally, influenced by the movement of the welding temperature field, the temperature gradient behind the electric arc axis along the length of the weld pool is smaller than that along the width, which leads to the increment in the half length of the pool being greater than that in the width of the pool. However, as the root gap increases, the molten metal spread above the groove enters the interior of the groove, resulting in a decreasing trend in the size of the topside welding pool, and the reduction speed in the width of the pool is higher than that in the length of the pool. The combined effect of the welding current and groove gap results in an increase in the half-length and a slight increase in the width of the pool, with the tail of the pool showing a slender and pointed shape. From full penetration to over-penetration, the area at the tail of the weld pool continues to increase and the degree of sharpness in the shape of the weld pool becomes more pronounced. This is because, as the welding current and root gap further increase, the phenomenon of overpenetration occurs. As the weld pool increases, its collapse also increases. With the combined effect of the current and gap, the area of the weld pool tail tends to increase. However, due to the insufficient increase in the weld pool width to offset the decrease in its width caused by the weld pool collapse, the weld width slightly decreases and the shape of the weld pool tail becomes sharper and slenderer.

According to the above statement, the topside parameters of the weld pool tail related to the penetration state mainly include: the length L_T of the weld pool tail, the width W of the weld pool, the area S_T of the weld pool tail, the length-to-width ratio L_T/W of the weld pool tail, the trailing angle α of the weld pool, the area coefficient C_{TS} of the weld pool tail, and the width coefficient C_{TW} of the weld pool tail, as shown in Figure 2. The shape parameters α, C_{TS}, and C_{TW} are defined as follows:

$$\begin{cases} \alpha = 2\tan^{-1}(W/(2L_T)) \\ C_{TS} = S_T/(L_T \cdot W) \\ C_{TW} = W_{L_T/2}/W \end{cases} \tag{11}$$

where $W_{L_T/2}$ is the width of the welding pool at the tail half-length, as shown in Figure 2.

The characteristic values of the weld pool describing various penetration states can be obtained through parameterization calculation. Thus, a decision information system for the penetration state under variable current and gap conditions is established, as shown in Table 1. The system is a dataset consisting of twenty-three samples, seven conditional attributes, and one decision attribute, where the decision attribute is the back width W_B of the weld seam.

Table 1. Decision information system for welding penetration status.

U	L_T	W	L_T/W	S_T	C_{TS}	α *	C_{TW}	W_B (mm)
x_1	203.5	227.4	0.895	34,264.2	0.740	58.39	0.818	0
x_2	227.1	246.4	0.922	40,220	0.718	56.96	0.795	0
x_3	287.2	279.0	1.029	55,542.4	0.693	51.84	0.766	0
x_4	388.2	303.2	1.280	77,677.8	0.659	42.67	0.703	0
x_5	380.7	294.6	1.295	70,471.8	0.628	42.31	0.663	3.44
x_6	209.2	230.4	0.909	35,064.8	0.728	57.69	0.794	0
x_7	228.2	241.6	0.945	39,214.6	0.711	55.80	0.781	0
x_8	284.5	276.8	1.028	54,364	0.690	51.89	0.753	0
x_9	349.9	286.6	1.221	63,152.8	0.630	44.54	0.654	3.39
x_{10}	356.5	286.8	1.243	61,489.8	0.601	43.82	0.611	4.72
x_{11}	198.2	195.4	1.015	25,912.6	0.669	52.58	0.722	2.09
x_{12}	229.0	222.6	1.029	33,977	0.667	51.84	0.708	2.42
x_{13}	285.1	256.2	1.113	47,002.4	0.643	48.41	0.661	3.09
x_{14}	356.1	272.4	1.307	58,891.8	0.607	41.88	0.620	4.31
x_{15}	393.9	264.2	1.492	62,363	0.599	37.07	0.606	5.15

Table 1. *Cont.*

U	L_T	W	L_T/W	S_T	C_{TS}	α *	C_{TW}	W_B (mm)
x_{16}	225.5	192.2	1.174	29,641	0.684	46.16	0.700	2.59
x_{17}	264.5	207.4	1.275	36,261.8	0.661	42.82	0.686	3.40
x_{18}	306.1	223.2	1.371	43,665	0.639	40.07	0.657	4.03
x_{19}	397.1	240.2	1.653	57,250	0.599	33.69	0.610	5.03
x_{20}	448.5	244.2	1.837	64,010	0.585	30.56	0.587	5.37
x_{21}	222.7	184.4	1.207	26,597	0.647	45.06	0.678	3.67
x_{22}	250.0	210.8	1.186	33,429.4	0.634	45.74	0.662	3.87
x_{23}	323.8	222.4	1.458	35,481.6	0.618	37.94	0.621	4.90

* Trailing angle of weld pool.

4.2. Acquisition for Classification Rules

Before using the VPRS algorithm to acquire knowledge from Table 1, discretization preprocessing is required for the continuous data in the table. For the conditional attributes, the FCM clustering algorithm is used to divide the continuous data into three categories, and the partitioning results are arranged in ascending order, represented as discrete values 1, 2, and 3. For the decision attribute W_B, it can be divided into three categories according to relevant classification standards: incomplete penetration, complete penetration, and over-penetration [32], represented by the discrete values 0, 1, and 2, respectively.

Using the ASBAR algorithm (Algorithm 1) for attribute reduction in Table 1, the results are shown in Figure 3, where the threshold $\beta = 0.8$. The significance $SIG(\cdot)$ of the weld pool features is arranged in descending order as follows:

$$SIG(C_{TW}) > SIG(C_{TS}) > SIG(L_T/W) > SIG(\alpha) = \cdots = SIG(L_T) = 0. \quad (12)$$

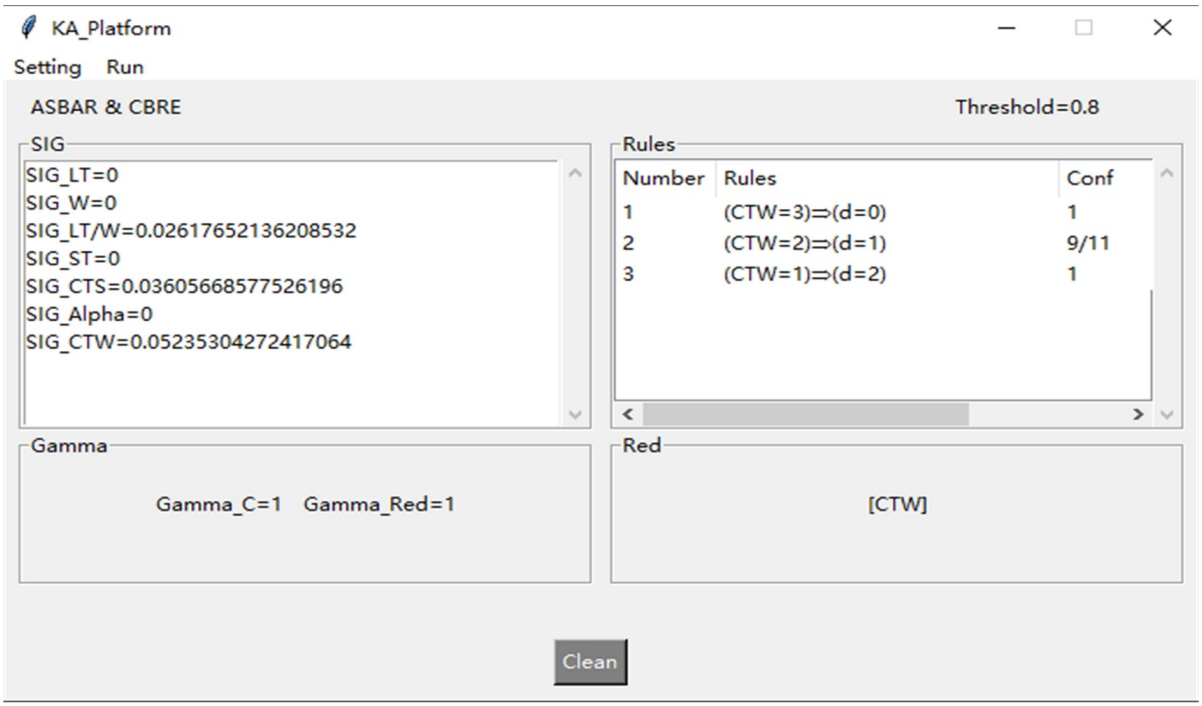


Figure 3. Knowledge acquisition results in the decision information system of welding penetration status.

It can be seen from Formula (12) that the width coefficient C_{TW} of the weld pool tail is the most important for determining the penetration state, followed by the area coefficient C_{TS} of the weld pool tail and the length-to-width ratio L_T/W of the weld pool tail. The importance of the remaining shape parameters is zero, which implies that from

the perspective of information entropy, removing these parameters from Table 1 has no impact on the classification results.

From the result of $\gamma_{RED} = \gamma_{C_{TW}} = \gamma_C = 1$ in Figure 3, the decision information system that retains only the feature parameter C_{TW} of the weld pool has the same classification ability as the unreduced decision information system. Therefore, $RED = \{C_{TW}\}$ is a minimal reduction in Table 1.

Set the threshold $\lambda = 0.8$. By using the CBRE algorithm (Algorithm 2) to extract rules from the reduced decision information system, we can obtain a set of classification rules R_i of the welding penetration state:

$$\begin{aligned} R_1: &\text{ If } C_{TW} = 3, \text{ then } W_B = 0(\text{conf} = 1) \\ R_2: &\text{ If } C_{TW} = 2, \text{ then } W_B = 1(\text{conf} = 9/11) \\ R_3: &\text{ If } C_{TW} = 1, \text{ then } W_B = 2(\text{conf} = 1) \end{aligned}$$

where the attribute values of C_{TW} and W_B correspond to "small", "medium", and "large" in ascending order, respectively, and conf is the confidence of a rule. From the above rules, there is a one-to-one correspondence between C_{TW} and W_B, and C_{TW} monotonically decreases as W_B increases.

4.3. Fuzzy Control Model and Reasoning

Based on the corresponding relationship between the width coefficient C_{TW} of the molten pool tail and the penetration state W_B, a fuzzy control model is established with C_{TW} as the control variable. The inputs are the error e and error change ec of C_{TW}, and the output is the welding current variation ΔI. The expectation value $\widetilde{C}_{TW} = 0.661$.

To establish the control rules, the language values of input and output are divided into three types, PB (positive big), ZE (zero), and NB (negative big). Because C_{TW} decreases with W_B and W_B increases with the welding current I, it can be inferred that C_{TW} monotonically decreases with I. Based on the general operating experience of welders, a set of control rules for the shape parameter C_{TW} of the weld pool can be given as follows.

$$\begin{aligned} \text{Rule 1}: &\text{ If } e = NB \text{ and } ec = NB, \text{ then } \Delta I = NB \\ \text{Rule 2}: &\text{ If } e = NB \text{ and } ec = ZE, \text{ then } \Delta I = NB \\ \text{Rule 3}: &\text{ If } e = NB \text{ and } ec = PB, \text{ then } \Delta I = ZE \\ \text{Rule 4}: &\text{ If } e = ZE \text{ and } ec = NB, \text{ then } \Delta I = NB \\ \text{Rule 5}: &\text{ If } e = ZE \text{ and } ec = ZE, \text{ then } \Delta I = ZE \\ \text{Rule 6}: &\text{ If } e = ZE \text{ and } ec = PB, \text{ then } \Delta I = PB \\ \text{Rule 7}: &\text{ If } e = PB \text{ and } ec = NB, \text{ then } \Delta I = ZE \\ \text{Rule 8}: &\text{ If } e = PB \text{ and } ec = ZE, \text{ then } \Delta I = PB \\ \text{Rule 9}: &\text{ If } e = PB \text{ and } ec = PB, \text{ then } \Delta I = PB \end{aligned}$$

The construction of a fuzzy membership function is a key aspect of modeling. There are more than ten methods to determine membership function, such as the intuitive method, Delphi method, and binary comparison sorting method [33]. However, most methods are difficult to apply in the occasions of welding process control due to subjective factors. Using the data derived from the $I \times G$ combination welding experiment, an algorithm minimizing fuzzy entropy is given to determine the fuzzy membership function of error e.

- Calculate the error e of C_{TW} from Table 1 to obtain a subset E' of the error universe E. Then, divide E' into the NB, ZE, and PB types of error using the fuzzy c-means (FCM) algorithm as shown in Table 2, where e_C is the clustering center for each type of error.

- Select the trapezoidal distribution as the membership function of E, as shown in Figure 4a, where $t_0 \in (-0.007, 0.023)$, $t_1 \in (0.092, 0.127)$, and $t_2 \in (-0.047, -0.04)$ are undetermined parameters.
- Establish the following optimization model with fuzzy entropy $H(\cdot)$ as a measure of fuzziness:

$$\min H(NB, ZE, PB) = \frac{1}{23 \ln 2} \sum_{i=1}^{23} (S(NB(e_i)) + S(ZE(e_i)) + S(PB(e_i))) \tag{13}$$

$$\text{s.t. } NB(e) = f(e, t_0, t_2),\ ZE(e) = g(e, t_0, t_1, t_2),\ PB(e) = h(e, t_1) \tag{14}$$

where $S(a) = -a \ln a - (1-a) \ln(1-a)$ for any $a \in [0, 1]$.

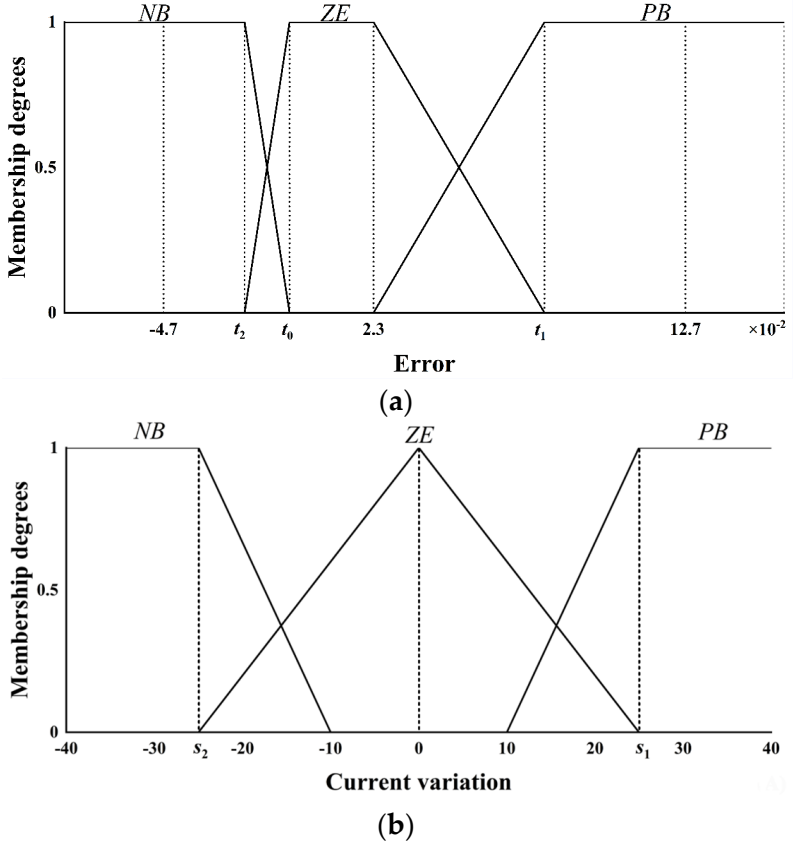


Figure 4. Membership functions of error (**a**) and current variation (**b**).

Table 2. Types of error and their clustering centers.

Type	e	e_C
NB	−0.074, −0.055, −0.051, −0.05, −0.041, −0.04	−0.047
ZE	−0.007, −0.004, 0, 0.001, 0.002, 0.017, 0.025, 0.04, 0.043, 0.047, 0.061	0.023
PB	0.092, 0.105, 0.121, 0.133, 0.134, 0.157	0.127

By minimizing the fuzzy entropy, it is obtained that $t_0 = -0.007$, $t_1 = 0.092$, and $t_2 = -0.04$. Thus, the membership function of error e is determined using the trapezoidal fuzzy distribution shown in Figure 4a. The membership function of the error change ec is the same as that of error e.

Let the membership function of the welding current variation ΔI be a triangular fuzzy distribution, as shown in Figure 4b, where s_1 and s_2 are undetermined parameters. From

"If e is ZE then ΔI is ZE" and "If e is PB then ΔI is PB", it can be inferred that there is a certain propositional relationship between ΔI and e, which satisfies

$$\Delta I = \varphi_I \cdot e = (s_1/t_1) \cdot e \tag{15}$$

where $\varphi_I = s_1/t_1$ is the regulation coefficient of welding current at $e = t_1$. From Table 1, it can be obtained that for $j = 1, 2, \cdots, n$,

$$\varphi_I^{(j)} = \left| (I_{PB}^{(j)} - I_{ZE}^{(j)}) / (e_{PB}^{(j)} - e_{ZE}^{(j)}) \right| \tag{16}$$

where $e_{PB}^{(j)}$ and $e_{ZE}^{(j)}$ are the errors of PB type and ZE type, respectively, and $I_{PB}^{(j)}$ and $I_{ZE}^{(j)}$ are the welding currents corresponding to $e_{PB}^{(j)}$ and $e_{ZE}^{(j)}$, respectively.

Let $\varphi_I = \max_{j=1}^{n} \varphi_I^{(j)}$. From Formulas (15) and (16), it gives that

$$s_1 = \max_{j=1}^{n} \left| (I_{PB}^{(j)} - I_{ZE}^{(j)}) / (e_{PB}^{(j)} - e_{ZE}^{(j)}) \right| \cdot t_1 \approx 28.$$

Analogously, it can be obtained that

$$s_2 = \max_{j=1}^{n} \left| (I_{NB}^{(j)} - I_{ZE}^{(j)}) / (e_{NB}^{(j)} - e_{ZE}^{(j)}) \right| \cdot t_2 \approx -22.$$

By experimental modification, $s_1 = 25$ and $s_2 = -25$ are taken, respectively.

Based on the given control rules, the output ΔI^* corresponding to the inputs e^* and ec^* is determined by using the Mamdani inference algorithm, as shown in Figure 5, where $e^* = 0.07$ and $ec^* = 0.02$.

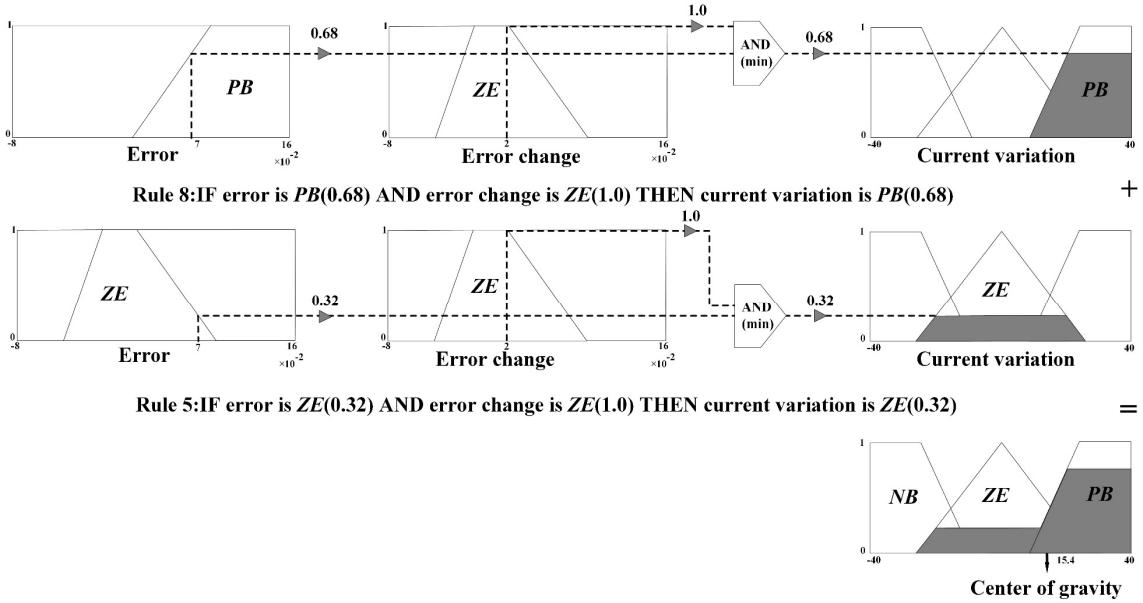


Figure 5. Reasoning procedures of the Mamdani algorithm.

4.4. Experiment Validation

In order to inspect the effectiveness of the rough-fuzzy control scheme for the penetration process, the following experiments are conducted based on the MAG welding platform. The main welding process parameters are the same as the $I \times G$ combination modeling experiment, with a CCD sampling interval of 400 ms.

Considering the changes in gaps during the welding process, the workpieces are processed and assembled to obtain two types of weldments, T1 and T2. The fit-up gap of T1 varies in steps from 1.2 to 0.6 to 1.2 mm, while the root gap of T2 gradually varies

from 0.4 to 2.0 mm, as shown in Figure 6. The welding experiments are conducted using constant current and rough-fuzzy control schemes, respectively. After welding, the back width of the weld seam is measured to evaluate the penetration status.

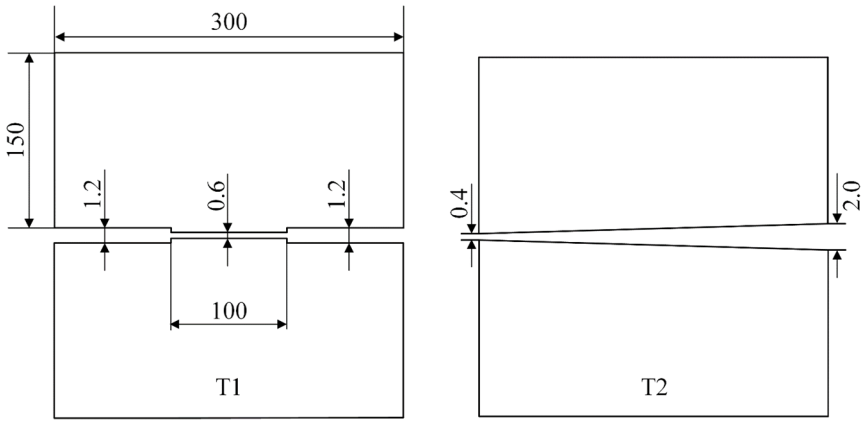
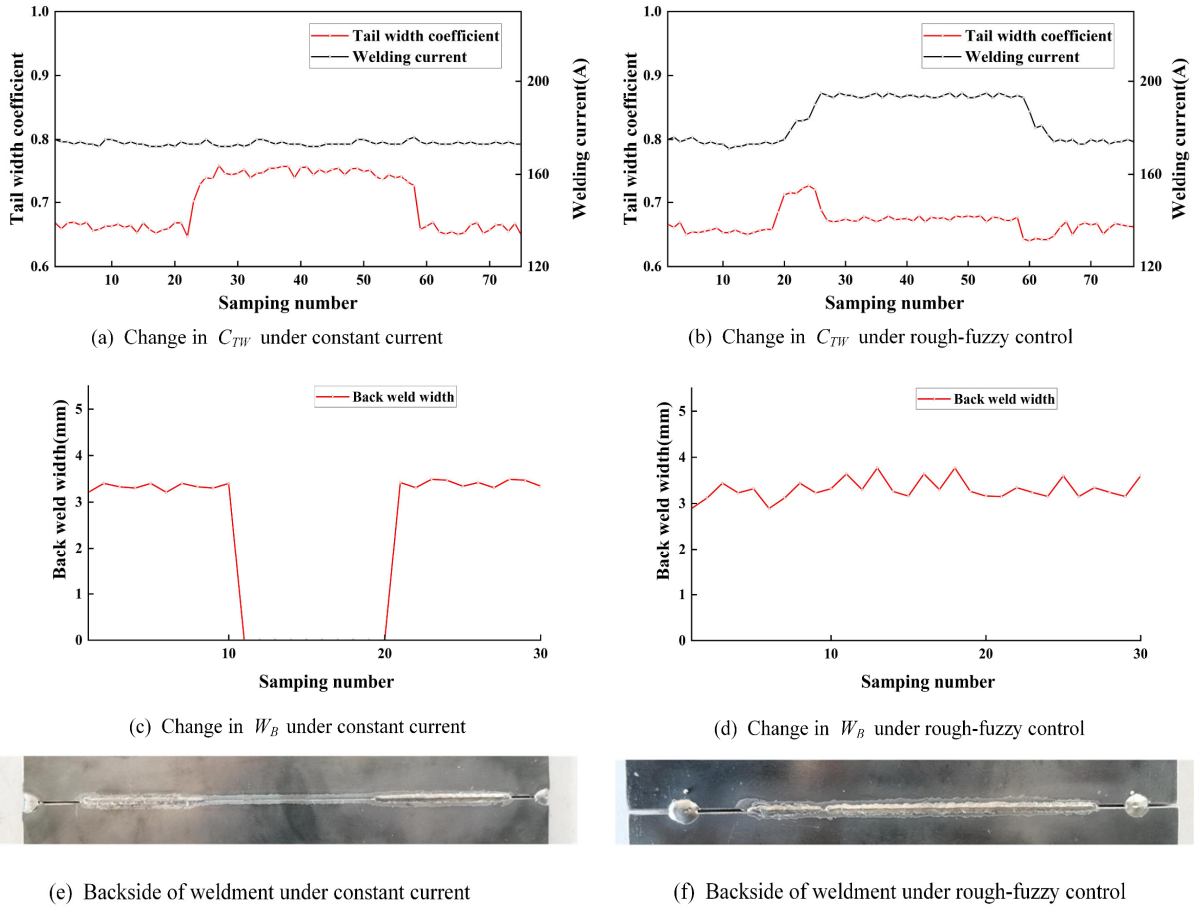


Figure 6. Changes in the fit-up gap of the T1 and T2 weldments.

For the T1 weldment, Figure 7a,c,e show the tail width coefficient C_{TW} of the weld pool, the back width W_B of the weld seam, and the backside of the weldment under constant current conditions. It can be seen that the C_{TW} value first increases and then decreases at the gap mutation, and the weld seam is in an incomplete penetration state at a gap of 0.6 mm. Figure 7b,d,f indicate the C_{TW}, the back width W_B of the weld seam, and the backside of the weldment under rough-fuzzy control conditions. Except for small fluctuations at the gap mutation, the C_{TW} value tends to stabilize, and the weld seam is totally penetrated.



(a) Change in C_{TW} under constant current

(b) Change in C_{TW} under rough-fuzzy control

(c) Change in W_B under constant current

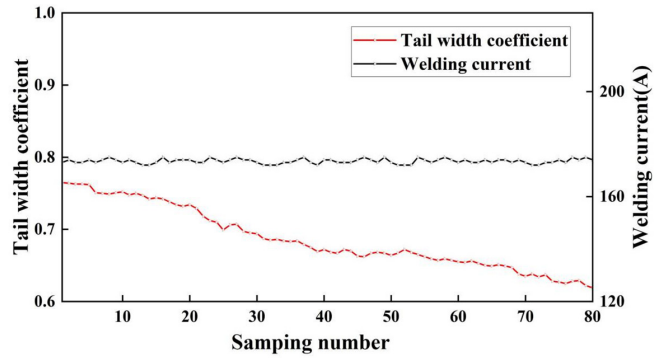
(d) Change in W_B under rough-fuzzy control

(e) Backside of weldment under constant current

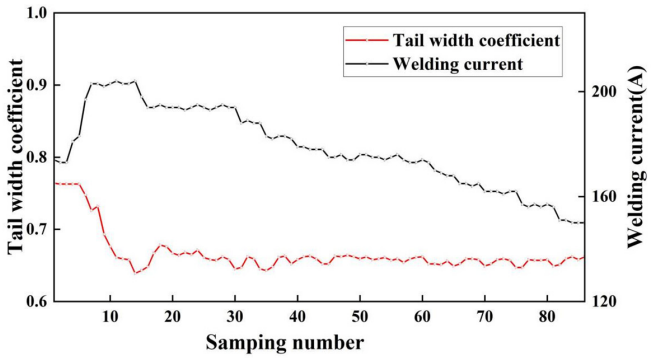
(f) Backside of weldment under rough-fuzzy control

Figure 7. Penetration state of T1 weldment under constant current and rough-fuzzy control.

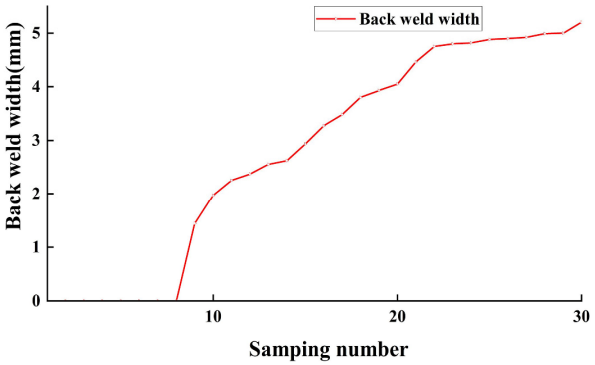
For the T2 weldment, Figure 8a,b show the changes in the tail width coefficient C_{TW} with the gap. It can be seen that the C_{TW} value decreases with the increase in the gap under constant current, while it tends to stabilize after an initial reduction under rough-fuzzy control. Figure 8c–f indicate the back width W_B of the weld seam and the backside of the weldment. For constant current welding, the weld seam gradually changes from incomplete penetration to full penetration and then to over-penetration. For closed-loop control, except for incomplete penetration in the initial stage, the weld seam is in a fully penetrated state, and the back width remains generally uniform and consistent.



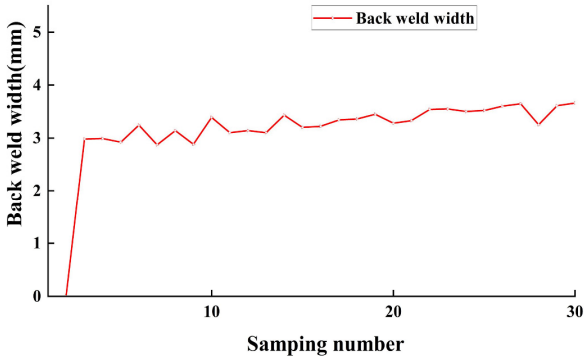
(a) Change in C_{TW} under constant current



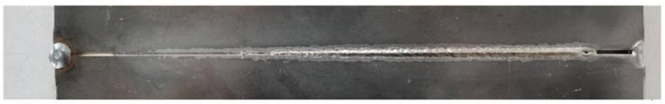
(b) Change in C_{TW} under rough-fuzzy control



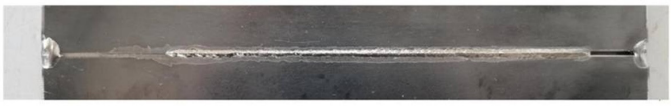
(c) Change in W_B under constant current



(d) Change in W_B under rough-fuzzy control



(e) Backside of weldment under constant current



(f) Backside of weldment under rough-fuzzy control

Figure 8. Penetration state of T2 weldment under constant current and rough-fuzzy control.

5. Conclusions

(1) By utilizing the changes in information entropy to define attribute importance, an attribute-significance-based approximate reduction algorithm is presented. The algorithm not only maintains the stability of the reduction process, but also helps to quickly derive a minimum feature set of the welding pool that characterizes the welding penetration state.

(2) Through the knowledge acquisition of the rough set, the change regularity of the topside features of the molten pool with the penetration state can be obtained from the dataset of $I \times G$ combination welding experiments. Therefore, in closed-loop control, it is not necessary to predict the penetration depth, but to implement penetration control by adjusting the topside shape of the weld pool.

(3) The welding experimental result indicates that the rough-fuzzy control scheme can effectively control the penetration state under variable gap conditions. The backside of the weld seam is well shaped and meets the requirements of the welding specifications.

Author Contributions: Conceptualization, Z.F.; methodology, Z.F.; software, H.Y.; validation, H.Y. and X.L.; formal analysis, J.H.; investigation, N.L.; resources, H.Y.; data curation, Q.L.; writing—original draft preparation, Z.F.; writing—review and editing, H.Y. visualization, J.H.; supervision, N.L.; project administration, Q.L.; funding acquisition, Z.F. All authors have read and agreed to the published version of the manuscript.

Funding: This work was supported by the National Natural Science Foundation of China under grant No. 51969001 and No. 52261044.

Data Availability Statement: Not applicable.

Acknowledgments: The authors appreciate the necessary technical support provided by the School of Materials Science and Engineering, Shanghai Jiao Tong University.

Conflicts of Interest: The authors declare no conflict of interest.

References

1. Duan, S.Y. *Fundamentals of Gas Shielded Welding Process*; Machine Press: Beijing, China, 2007.
2. Wu, L.; Chen, S.B. *Intelligent Technology of Arc Welding Robot*; National Defence Industry Press: Beijing, China, 2000.
3. Wang, K.H. *Research on Feature Extraction and Intelligent Control of Molten Pool Based on Vision*; Nanjing University of Science & Technology: Nanjing, China, 2007.
4. Fan, C.J. *Weld Pool Characters Extraction Visual Sensing and Intelligent Control during Varied Gap Aluminum Alloy Pulsed GTAW Process*; Shanghai Jiaotong University: Shanghai, China, 2008.
5. Pawlak, Z. *Rough Sets: Theoretical Aspects of Reasoning about Data*; Kluwer Academic Publishing: Dordrecht, The Netherlands, 1991.
6. Yu, J.H. *On Rough Set-Based Knowledge Discovery and Decision-Making Methods for Some Generalized Information Systems*; Harbin Institute of Technology: Harbin, China, 2020.
7. Zhang, X.F.; Lin, X.F. Automatic machine learning algorithm based on rough set theory. *J. Shenyang Univ. Nat. Sci.* **2022**, *36*, 468–477.
8. Chen, Z.J.; Tan, J.P.; Shi, L.X.; Xue, S.H.; Huang, T.R. Impact pattern recognition between sliding tank ear and tank track under unbalanced load state of the cage. *Noise Vib. Control* **2019**, *39*, 203–208.
9. Feng, Y.; Gao, X.; Zhang, Y.; Peng, C.; Gui, X.; Sun, Y.; Xiao, X. Simulation and Experiment for dynamics of laser welding keyhole and molten pool at different penetration status. *Int. J. Adv. Manuf. Technol.* **2021**, *112*, 2301–2312. [CrossRef]
10. Ye, G.; Gao, X.; Liu, Q.; Wu, J.; Zhang, Y.; Gao, P.P. Prediction of weld back width based on top vision sensing during laser-MIG hybrid welding. *J. Manuf. Process.* **2022**, *84*, 1376–1388. [CrossRef]
11. Saha, A.; Reddy, J.; Kumar, R. A fuzzy similarity based classification with Archimedean-Dombi aggregation operator. *J. Intell. Manag. Decis.* **2022**, *1*, 118–127. [CrossRef]
12. Puška, A.; Stojanović, I. Fuzzy multi-criteria analyses on green supplier selection in an agri-food company. *J. Intell. Manag. Decis.* **2022**, *1*, 2–16. [CrossRef]
13. Darwito, P.A.; Indayu, N. Adaptive neuro-fuzzy inference system based on sliding mode control for quadcopter trajectory tracking with the presence of external disturbance. *J. Intell. Syst. Control* **2023**, *2*, 33–46. [CrossRef]
14. Su, J.F.; Xu, B.J.; Li, L.C.; Wang, D.; Zhang, F.T. A green supply chain member selection method considering green innovation capability in a hesitant fuzzy environment. *Axioms* **2023**, *12*, 188. [CrossRef]
15. Wu, D.; Liao, Y.; Hu, C.; Yu, S.; Tian, Q. An enhanced fuzzy control strategy for low-level thrusters in marine dynamic positioning systems based on chaotic random distribution harmony search. *Int. J. Fuzzy Syst.* **2021**, *23*, 1823–1839. [CrossRef]
16. Marji Harly, M. Design of low jerk automatics transmission for vehicle using fuzzy control to improve gear shifting quality and low fuel consumption. In Proceedings of the 3rd International Conference on Vocational Education of Mechanical and Automotive Technology (ICoVEMAT), Yogyakarta, Indonesia, 5 October 2020.
17. Urrea, C.; Kern, J.; Alvarado, J. Design and evaluation of a new fuzzy control algorithm applied to a manipulator robot. *Appl. Sci.* **2020**, *10*, 7482. [CrossRef]
18. Gao, F.X. Vision-based curve tracking system using fuzzy controller. *Control Eng. China* **2016**, *23*, 149–152.
19. Zou, Y.B.; Wang, Y.B.; Zhou, W.L. Line laser visual servo control system for seam tracking. *Opt. Precis. Eng.* **2016**, *24*, 2689–2698.
20. Lu, J.Y.; Zhu, D. Control system design of adaptive welding seam tracking. *Weld. Join.* **2018**, *9*, 61–65.
21. Wang, Z.; Wang, X.; Gao, W.X.; Wang, Y.K. Research fuzzy incremental control submerged arc weld with image processing. *Meas. Control Technol.* **2016**, *35*, 70.
22. Wu, Y.Q.; Yuan, Z.H.; Wang, J.H. A fuzzy controller design of seam tracking for welding robot. *Adv. Mater. Res.* **2012**, *442*, 370–374. [CrossRef]

23. Wang, P.C.; Zhang, D.F.; Lu, B.C. Robust fuzzy sliding mode control based on low pass filter for the welding robot with dynamic uncertainty. *Ind. Robot. Int. J. Robot. Res. Appl.* **2020**, *47*, 111–120. [CrossRef]
24. Chen, Q.; Pan, J.L.; Oshima, K. Fuzzy control in welding process. *Chin. J. Mech. Eng.* **1995**, *31*, 86–91.
25. Chen, S.B.; Lou, Y.J.; Zhao, D.B.; Wu, L. Fuzzy-neural network modeling and control of pool dynamic process in pulsed GTAW. *Acta Autom. Sin.* **2002**, *28*, 74–82.
26. Pan, Q. *Visual Sensing of Fusion Hole and Penetration Close-Loop Control in Thin Plate High Frequency Pulsed TIG Welding*; Shangdong University: Jinan, China, 2022.
27. Jiang, Z.; Lu, S.Y.; Yu, S.W.; Zhang, Q.; Li, Z.P. Design of steel mesh welding control system based on PLC and fuzzy control algorithm. *Comput. Era* **2022**, *12*, 106–111.
28. Wang, W.D.; Wang, Z.J.; Hu, S.S.; Xue, K.X.; Zhao, G.C. Adaptive predictive control of weld penetration depth based on Hammerstein model in pulsed gas metal arc welding. *J. Mech. Eng.* **2019**, *55*, 138–145. [CrossRef]
29. Wu, D. *Research on Predicting and Intelligent Control for Weld Formation during VPPAW Process Using Multi-Information Fusion*; Shanghai Jiao Tong University: Shanghai, China, 2018.
30. Ziarko, W. Variable precision rough set model. *J. Comput. Syst. Sci.* **1993**, *46*, 39–59. [CrossRef]
31. Wang, G.Y.; Yu, H.; Yang, D.C. Decision table reduction based on conditional information entropy. *Chin. J. Comput.* **2002**, *25*, 759–766.
32. Liu, M. *Research on Process and Control Method Based on Visual Sensing of the MAG Weld during One-Side Welding with Back Free Formation*; Nanjing University of Science & Technology: Nanjing, China, 2012.
33. Liang, R.R.; Pan, X.D. The determination method and experimental research of the membership function of fuzzy set. *J. Sichuan Norm. Univ. Nat. Sci.* **2021**, *44*, 479–486.

Disclaimer/Publisher's Note: The statements, opinions and data contained in all publications are solely those of the individual author(s) and contributor(s) and not of MDPI and/or the editor(s). MDPI and/or the editor(s) disclaim responsibility for any injury to people or property resulting from any ideas, methods, instructions or products referred to in the content.